Novel Phases in the Field Induced Spin Density Wave State in $(TMTSF)_2PF_6$

A. V. Kornilov[a], V. M. Pudalov[a], Y. Kitaoka[b], K. Ishida[b], T. Mito[b], J. S. Brooks[c], J. S. Qualls[c], J. A. A. J. Perenboom[d], N. Tateiwa[e], T. C. Kobayashi[e]

[a)] *P. N. Lebedev Physics Institute, 117924 Moscow, Russia.*

[b)] *Division of Material Physics, School of Engineering Science, Osaka University, Toyonaka, Osaka 560-8531, Japan*

[c)] *National High Magnetic Field Laboratory, Florida State University, Talahasse FL 32310 USA*

[d)] *High Field Magnet Laboratory, University of Nijmegen, NL-6525 ED Nijmegen, The Netherlands*

[e] *Research Center for Materials Science at Extreme Condition, Osaka University, Toyonaka, Osaka 560-8531, Japan*

(February 1, 2008)

Magnetoresistance measurements on the quasi one-dimensional organic conductor $(TMTSF)_2PF_6$ performed in magnetic fields B up to 16 T, temperatures T down to 0.12 K and under pressures P up to 14 kbar have revealed new phases on its $P-B-T$ phase diagram. We found a new boundary which subdivides the field induced spin density wave (FISDW) phase diagram into two regions. We showed that a low-temperature region of the FISDW diagram is characterized by a hysteresis behavior typical for the first order transitions, as observed in a number of studies. In contrast to the common believe, in high temperature region of the FISDW phase diagram, the hysteresis and, hence, the first order transitions were found to disappear. Nevertheless, sharp changes in the resistivity slope are observed both in the low and high temperature domains indicating that the cascade of transitions between different subphases exists over all range of the FISDW state. We also found that the temperature dependence of the resistance (at a constant B) changes sign at about the same boundary. We compare these results with recent theoretical models.

Layered organic compounds tetramethiltetraselenafulvalene $(TMTSF)_2X$, where the anion X is ClO_4, AsF_6, PF_6 etc are unique material systems with a very rich phase diagram (for a review see Refs. [1–4]). Conduction in this materials is highly anisotropic, with ratio of the components $\sigma_{xx} : \sigma_{yy} : \sigma_{zz} \sim 10^5 : 10^3 : 1$. At ambient pressure, below temperature of 12 K, the PF_6-compound becomes dielectric with antiferromagnetic spin ordering in the spin density wave state. As pressure increases, the temperature of the antiferromagnetic ordering decreases and at about $P = 6$ kbar a superconducting state sets in. Magnetic field B applied in the least conducting direction z, first quenches the superconducting state and, further induces a cascade of phase transitions between FISDW states accompanied by the quantum Hall effect [5,6].

A so called 'standard' model was suggested [1,2,7] to explain the metal-SDW transition in magnetic field. Later it was developed into a 'Quantized Nesting Model' in Refs. [8–11] to describe a cascade of the first order transitions between different FISDW sub-phases. According to this model, electrons condense in the SDW state whose period determines a nesting vector in the momentum space. Under the assumption of the electron-hole symmetry, $x-$component of the nesting vector Q_x is quantized as [8,3]

$$Q_x = 2k_F - N\frac{eBb}{h}, \qquad (1)$$

where k_F is Fermi wave vector, b is the size of the elementary cell in $y-$ direction, and N is an integer. As magnetic field varies, N changes by an integer, causing step-like changes in the nesting vector, which result in the sequence of the first-order phase transitions.

According to the recent analysis [12], however the electron-hole symmetry in the SDW state is not fulfilled unless $N = 0$ in Eq. (1). As a result, (i) the nesting vector is not strictly quantized and (ii) the step-like changes in the nesting vector may disappear above a certain temperature transforming into oscillations. Correspondingly, as temperature increases, the first order transitions with $\Delta N \approx 1$ may disappear, whereas FISDW state still persists. Thus, in contrast to the 'Quantized Nesting Model' which predicts the first order phase transition to exist over the whole range of temperatures where FISDW develops, the 'novel model' predicts the first order phase transitions may disappear above a certain temperature, T_0. The latter possibility depends on the parameter $\hbar\omega_c/(2\pi k_B T_0)$ [12], where ω_c is the cyclotron frequency.

In order to verify the theoretical predictions of the two models above, we studied temperature dependence of the magnetoresistance in $(TMTSF)_2PF_6$ at various pressures. Specifically, we measured, at different pressures, a temperature evolution of the hysteresis intrinsic to magnetoresistance traces of $R(B)$. We observed that the hysteresis indeed disappears above a temperature T_0 whereas FISDW state still persists. We found such behavior to manifest itself over the whole explored range of the existence of the FISDW. According to our results, the total $P-B-T$ phase diagram of the FISDW state can be subdivided into two domains, the 'low-T' domain where the first order phase transitions between FISDW sub-phases take place, and the 'high-T' domain where the transitions between the FISDW states do not exhibit first order behavior. This observation is in agreement with the 'novel model'; in the latter case, the 'low T-phase' is treated as a 'quantum FISDW' state with step-like changes in the

nesting vector, whereas the 'high T-phase' is treated as the 'semi-classical FISDW' state where the nesting vector oscillates. We also found that as temperature decreases and crosses the boundary between the two domains, the behavior of the resistivity changes qualitatively, from ordinary insulating-like ($dR/dT < 0$) through the 'high-T'-domain, to the metallic-like ($dR/dT > 0$) through the 'low-T'-domain. Around the $T = T_0$-boundary, $R(T)$ exhibits a maximum.

Experimental. Three samples (of a typical size $2 \times 0.8 \times 0.3\,\mathrm{mm}^3$) were grown by a conventional electrochemical technique. Measurements were made using either four Ohmic contacts formed at the $a-b$ plane or eight contacts at two $a-c$ planes; in all cases 25μm Pt-wires were attached by a graphite paint to the sample along the most conducting direction a. The sample and a manganin pressure gauge were inserted into a Teflon cylinder placed inside a nonmagnetic 18 mm o.d. pressure cell [13] filled with Si-organic pressure transmitting liquid. The cell was mounted inside the liquid He^4, He^3, or He^3/He^4 chamber, in a bore of a 16 T superconducting magnet. For all measurements, the magnetic field was applied along the least conducting direction, z, of the crystal. Sample resistance was measured by four probe ac technique at 132 Hz frequency, with current 1-4 μA to avoid nonlinear effects. The out-of phase component of the measured voltage was found to be negligible in all measurements, indicating Ohmic contacts to the sample.

The sample temperature was varied slowly, at a rate less than 0.25 K/min in order to avoid breaking the sample. The measured changes in the sample resistance were fully reproducible during the full run of measurements including temperature sweeps; this indicated that the sample quality did not change. The magnetoresistance was measured either at a constant T and varying magnetic field B, or at a constant B and varying T. Sample temperature was determined by RuO_2 resistance thermometer with a pre-calibrated magnetoresistance. Measurements were done in magnetic fields up to 16 T and for temperatures in the range from 1.4 to 30 K (mainly) and down to 0.12 K (partly). The most detailed results were obtained for pressures 7, 8, 10 and 14 kbar.

Figure 1 shows magnetoresistance traces measured (a) at $P = 10$ kbar in the temperature range 0.6-4.2 K and (b) at 8 kbar, 0.12 K. In agreement with earlier observations [14], when magnetic field exceeds the critical value (which is 0.16 T in our case), the superconductivity is quenched and the sample resistance starts gradually increasing. Further, this smooth dependence transforms into step-like changes in R. As temperature decreases, the step-like changes become steeper and appear at progressively lower fields. This behaviour is also consistent with earlier observations [15,16,5,6] and is interpreted as transitions between different sub-phases in FISDW [17,6,5]. This interpretation is further supported by the hysteresis between $R(B)$ traces for the field ramping up and down, which is clearly seen in Fig. 1. The hysteresis is also consistent with earlier observations [6] and signals the onset of the first order phase transitions.

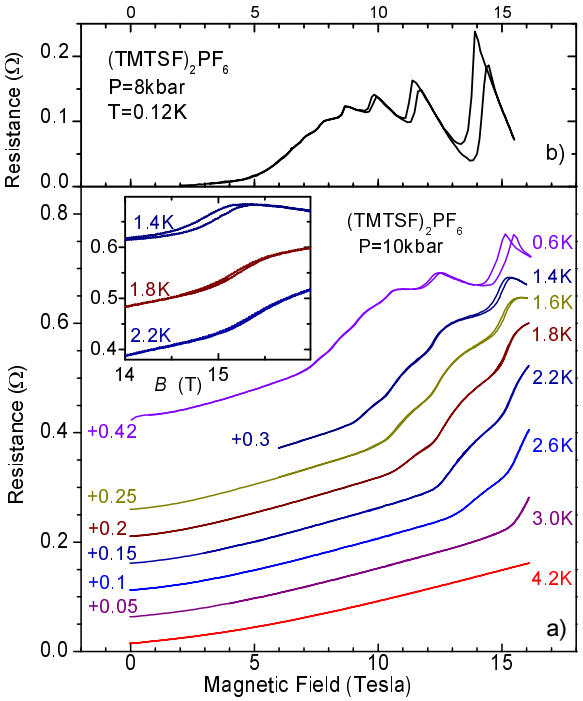

FIG. 1. Magnetoresistance R_{xx} vs magnetic field B_z: a) For $P = 10$ kbar and for eight temperatures (indicated for each curve). The curves are shifted vertically, for clarity (the offset values are indicated on the left side). The inset magnifies the temperature evolution of the hysteresis regions of $R(B)$-curves near $B = 15$ T. b) For $P = 8$ kbar and $T = 0.12$ K.

As temperature increases, the hysteresis weakens and tends to disappear as illustrated in the inset to Fig. 1 a. Nevertheless, the steps in $R(B)$ persist to higher temperatures, being therefore non- or at least partly correlated with the hysteresis. In order to quantify the hysteresis strength, we calculated the maximal width of the hysteresis loop δB for each curve and plotted it in Fig. 2 as a function of temperature; in this determination, the L/R time constant of the magnet was carefully measured and taken into account.

For three groups of the data in Fig. 2 the hysteresis width decreases linearly with temperature and vanishes at a certain temperature T_0; above $T = T_0$ it remains equal to zero. The falling part of these dependences were fitted with linear curves (solid lines), which appear to have the same slope. We plotted linear curves with the same slope through other single data points (dashed lines) in order to estimate T_0 for all transitions at different pressure values.

Measurements at two other pressures, 7 and 14 kbar have shown qualitatively similar results. At $P = 7$ kbar the steps (transitions) shift to lower fields and persist

up to higher temperatures. The hysteresis, δB, is bigger than that at 8 and 10 kbar and disappears at slightly higher temperature. At $P = 14$ kbar, the trend is opposite: T_0 becomes lower than that for 10 kbar.

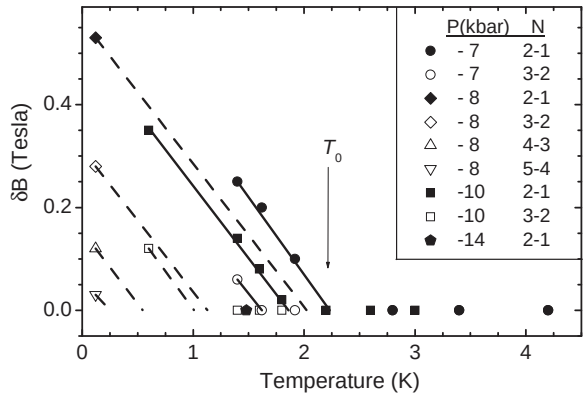

FIG. 2. Hysteresis width vs temperature for several pressures. Lines are the guide to the eye. Dashed lines show an anticipated behavior in cases where only single data point was taken. The table shows pressure values P (in kbar) and the sub-phase numbers N between which the transition takes place. Vertical arrow depicts T_0 for one of the transitions, $N = 2 \longleftrightarrow 1$ at $P = 7$ kbar.

The above three features, (i) the existence of the hysteresis in $R(B)$ at low temperature, (ii) its disappearance above a certain temperature T_0 and (iii) the persistence of the steps in $R(B)$ to temperatures higher than T_0, are observed in our experiments for several transitions (see Figs. 1, 2). It seems likely that these features are generic also to other transitions in the FISDW part of the phase diagram and that the hysteresis for higher N-values was not observed in our measurements just because T_0 for these transitions is lower than our lowest accessible temperature, 1.4 K (for the majority of measurements).

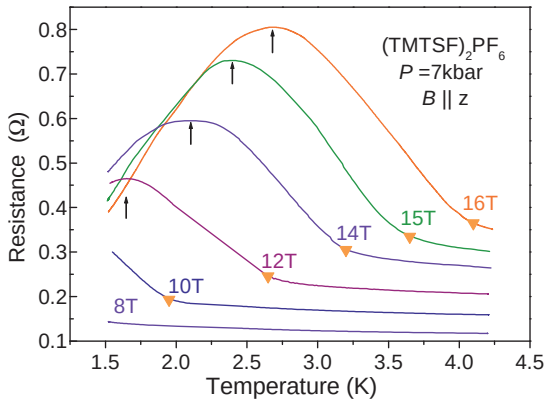

FIG. 3. Temperature dependences of the resistance for six different values of the magnetic field at pressure $P = 7$ kbar. Triangles depict the onset of the transitions. Arrows point the maximum in each curve at $T_{\max}$.

Figure 3 represents the results of temperature sweeps taken at six fixed magnetic fields for $P = 7$ kbar. Starting from high temperatures, the resistance increases as T decreases, then passes through a maximum at a certain temperature $T_{\max}$ and further decreases towards low temperatures. Triangles mark the onset of the phase transition at each curve. The similar $T-$dependences measured at $P = 10$ and 14 kbar were qualitatively similar to those shown in Fig. 3 but shifted to lower temperatures.

$B - T$ phase diagram in Fig. 4 summarizes the results of all measurements, at $P = 7$ kbar (the main panel) and at $P = 10$ kbar (the inset). The closed squares depict the onsets of the steps in $R(B)$ obtained from magnetic field sweeps at fixed temperatures and triangles are for the temperature sweeps $R(T)$ at fixed field. In addition to the data taken directly, the open squares show the lower temperature data, $T = 0.12$ K, taken at $P = 8$ kbar which has been recalculated to correspond to the data at $P = 7$ kbar (main panel) and to 10 kbar (inset). In this procedure, the data for 8 kbar were shifted in magnetic field according to the pressure coefficient $d(B^{-1})/dP = -0.015\,\mathrm{T}^{-1}\mathrm{kbar}^{-1}$ which we determined from the higher temperature data at $T = 1.4$ K for $P = 7$, 10, and 14 kbar. The hysteresis width is obtained from Fig. 2 and is depicted by the split lines.

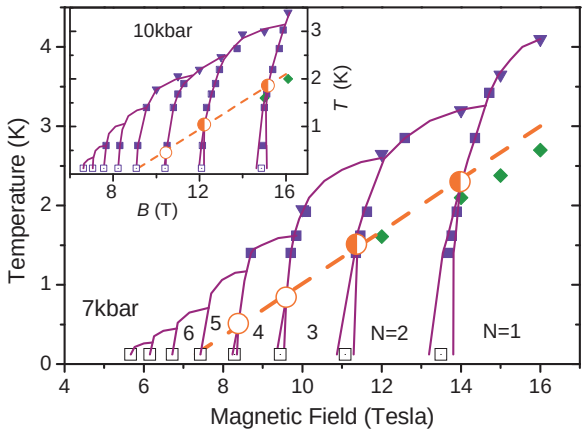

FIG. 4. $B - T$ – phase diagram for $P = 7$ kbar (main panel), and for $P = 10$ kbar (inset). Solid squares (triangles) correspond to the onset of the steps in $R(B)$ ($R(T)$) curves measured directly at the specified pressure ($P = 7$ and 10 kbar, correspondingly). Open squares are recalculated from the data taken at $P = 8$ kbar. Circles denote T_0: semi-closed symbols are for the data measured directly at the specified pressure, open ones are recalculated from the data measured at $P = 8$ kbar. Diamonds designate the temperature $T_{\max}$ of maxima in $R(T)$ measured directly at the specified pressure (see Fig. 3 for $P = 7$ kbar). Split lines of the phase diagram correspond to the hysteresis width; all other lines are guide to the eye.

In general, the $P - B - T$ phase diagram in Fig. 4 is qualitatively similar to that previously reported [6,5], but, in addition, displays the boundaries of hysteresis

domains vs temperature. The hysteresis domains for different transitions collapse above $T = T_0$; this was determined for seven transitions and the corresponding points are denoted with open circles. The separatrix points T_0 thus subdivide the phase boundaries into the two regions: the low temperature domain ($T < T_0$) of the hysteretic behaviour and the high temperature domain ($T > T_0$) where the FISDW transitions develop without a hysteresis. The disappearance of the hysteresis with rising temperature at one fixed pressure was mentioned earlier [6] but to the best of our knowledge no studies of this effect followed. The subdivison of the phase diagram is qualitatively consistent with the 'novel model' for the FISDW [12], where the low-temperature domain corresponds to the 'quantum FISDW' sub-phase and the high temperature domain corresponds to the 'semiclassical FISDW'. According to the model, in the former sub-phase the transitions between different phases take place with jumps in the nesting vector, are of the first order, and are accompanied by hysteresis of various physical quantities. In the latter sub-phase, the transitions between different phases take place without any jumps in the nesting vector, and are therefore not first order phase transitions.

The $B-T$ phase diagram on the main panel in Fig. 4 is plotted for pressure of 7 kbar. For $P = 10$ kbar (inset), the phase diagram looks qualitatively similar but the new phase boundary is shifted to lower temperature by about (0.5 - 1) K.

The dashed line in Fig. 4 connects the T_0-values (circles). In order to check whether the dashed line splits not only the phase boundaries but the overall $B-T$ parameter space, we plotted onto the same phase diagram the B, T-coordinates of the maxima on $R(T)$ curves from $T-$sweeps similar to that shown in Fig. 3.

The maxima in $R(T)$ dependences in the FISDW regime were observed earlier [20,21] and were associated with a non-linear temperature dependence of the σ_{xy} caused by the transition from the QHE to metallic regime [20,22,21]. In this interpretation, the maxima should correspond to the onset of the QHE regime. On the other hand, the hysteresis behaviour if associated with jumps in the nesting vector [12], should manifest in the QHE regime only. Therefore, T_{max} is expected to be $\leq T_0$. It is surprising that in our case $T_{\max}$ almost coincide with T_0 for different pressures, even though T_0 varies with pressure.

To summarize, from studies of the temperature and magnetic field dependences of the resistivity of the quasi-1D organic conductor, we found that its $P-B-T$ phase diagram splits in two domains, where the transitions between different FISDW states take place (i) with a hysteresis as the first order phase transitions (for low temperatures), and (ii) without hysteresis (for high temperatures). This result is not expected within the 'Quantized nesting model' and is consistent with the recent suggestion by Lebed [12] that the period of the spin structure in FISDW state can be either partially quantized or not quantized at all. We experimentally plotted the new phase boundary where such behavior occurs. We found that the $P-B-T$ boundary separating the two domains almost coincides with a line at which the dR/dT changes sign.

ACKNOWLEDGMENTS

A. V. K. and V. M. P. are grateful to A. G. Lebed and V. M. Yakovenko for fruitful discussions. The work was partially supported by INTAS, RFBR, NATO, NSF, NWO, Programs "Statistical physics", "Integration", "The State support of the leading scientific schools", and COE Research in Grant-in-Aid for Scientific Research, Japan.

[1] L. P. Gor'kov and A. G. Lebed, J. Phys. (Paris) Lett. **45**, L-433 (1984).
[2] L. P. Gor'kov Sov. Phys. Usp. **27**, 809 (1984).
[3] T. Ishiguro, K. Yamaji and G. Saito, Organic Superconductors (2nd Edition, Springer-Verlag, Heidelberg, 1998).
[4] P. M. Chaikin J. Phys I France **6**, 1875 (1996).
[5] S. T. Hannahs, J. S. Brooks, W. Kang, L. Y. Chiang and P. M. Chaikin Phys. Rev. Lett. **63**, 1988 (1989)
[6] J. R. Cooper, W. Kang, P. Auban, G. Montambaux and D. Jérome Phys. Rev. Lett. **63**, 1984 (1989).
[7] P. M. Chaikin, Phys. Rev. B **31**, 4770 (1985).
[8] M. Heritier, G. Montambaux and P. Lederer, J. Phys (Paris) Lett. **45**, L-943 (1984).
[9] A. G. Lebed, Sov. Phys. JETP, **62**, 595 (1985).
[10] K. Maki, Phys. Rev. B **33**, 4826 (1986).
[11] K. Yamaji, Synth. Met. **13**, 29 (1986).
[12] A. G. Lebed, JETP Lett. **72**, 141 (2000).
[13] A. V. Kornilov, V. A. Sukhoparov, V. M. Pudalov, *High Pressure Science and Technology*, ed. W. Trzeciakowski, World Scientific, Singapore, 63 (1996).
[14] R. L. Greene, P. Haen, S. Z. Huang et al., Mol. Cryst. Liq. Cryst. **79**, 225 (1982)
[15] P. M. Chaikin, Mu-Yong Choi, J. F. Kwak et al., Phys. Rev. Lett. **51**, 2333 (1983).
[16] M. Ribault, D. Jérome, D. Tuchender et al., J. Phys. (Paris) Lett. **44**, L-953 (1983).
[17] J. F. Kwak, J. E. Schirber, R. L. Green, E. M. Engler, Phys. Rev. Lett. **46**, 1296 (1981).
[18] J. P. Ulmet, P. Auban, A. Khmou et al., J. Phys. (Paris) Lett. **46**, L-545 (1985)
[19] R. L. Greene, E. M. Engler, Phys. Rev. Lett. **45**, 1587 (1980)
[20] W. Kang, S. T. Hannahs, L. Y. Chiang, R. Upasani, P. M. Chaikin, Phys. Rev. B **45**, 13566 (1992).
[21] T. Vuletić et al. preprint: cond-mat/0010106.
[22] V. M. Yakovenko, H.-S. Goan, Phys. Rev. B **58**, 10648 (1998).